IOPscience iopscience.iop.org

Home Search Collections Journals About Contact us My IOPscience

Magnetic properties of $Pr_{1-x}Gd_xMn_2Ge_2$

This article has been downloaded from IOPscience. Please scroll down to see the full text article.

2004 J. Phys.: Condens. Matter 16 405

(http://iopscience.iop.org/0953-8984/16/3/017)

View the table of contents for this issue, or go to the journal homepage for more

Download details:
IP Address: 129.252.86.83
The article was downloaded on 28/05/2010 at 07:51

Please note that terms and conditions apply.

INSTITUTE OF PHYSICS PUBLISHING JOURNAL OF PHYSICS: CONDENSED MATTER

J. Phys.: Condens. Matter **16** (2004) 405–414 PII: S0953-8984(04)70770-5

Magnetic properties of $Pr_{1-x}Gd_xMn_2Ge_2$

Y Elerman[1], I Dincer[1], A Elmali[1,4], H Ehrenberg[2], H Fuess[2], E Duman[3] and M Acet[3]

[1] Faculty of Engineering, Department of Engineering Physics, Ankara University, 06100 Besevler-Ankara, Turkey
[2] Institute for Materials Science, Darmstadt University of Technology, Petersenstrasse 23, D-64287 Darmstadt, Germany
[3] Experimentalphysik, Universität Duisburg-Essen, D-47048 Duisburg, Germany

E-mail: elmali@eng.ankara.edu.tr

Received 17 October 2003
Published 9 January 2004
Online at stacks.iop.org/JPhysCM/16/405 (DOI: 10.1088/0953-8984/16/3/017)

Abstract

The structural and magnetic properties of $Pr_{1-x}Gd_xMn_2Ge_2$ were studied by x-ray diffraction and magnetization measurements. The substitution of Gd for Pr leads to a linear decrease in the lattice constants and the magnetic interactions in the Mn sublattice cross over from a ferromagnetic character to an antiferromagnetic one. At low temperatures, the rare-earth sublattice also orders and reconfigures the ordering in the Mn sublattice. The spins in the Mn sublattice are arranged parallel to the Pr sublattice and antiparallel to the Gd sublattice. The results are collected in a phase diagram.

1. Introduction

Intermetallic layer-like compounds containing localized rare-earth (R) moments and the 3d transition element manganese exhibit interesting magnetic properties. Among ternary intermetallic compounds, one of the largest and most diverse groups is RMn_2X_2 compounds with R being a rare-earth and X Ge or Si [1, 2]. The magnetic phase diagram of the naturally layered intermetallic RMn_2X_2 compounds exhibits a wide variety of magnetic phenomena as a function of temperature and R. Ternary RMn_2X_2 compounds crystallize in the body-centred tetragonal $ThCr_2Si_2$-type structure (space group $I4/mmm$), which is characterized by stacked R–X–Mn–X–R layers along the c axis [3]. The magnetic structure of these compounds contains two interacting magnetic subsystems. One of them is composed of rare-earth atoms and manganese atoms form the other. According to the results of these investigations [1, 4], the *intra*layer Mn–Mn exchange interaction is the strongest, leading to a ferromagnetic coupling of the Mn moments along the c axis. On the other hand, the *inter*layer Mn–Mn exchange is very sensitive to the lattice parameter a, leading to ferromagnetic or antiferromagnetic ordering of

[4] Author to whom any correspondence should be addressed.

 © 2004 IOP Publishing Ltd Printed in the UK

the Mn sublattice, depending on the specific R element and temperature. The compounds with light rare earths (R = La–Nd) exhibit parallel alignment of Mn moments along the *c* axis below the Curie temperature T_C^{inter} and an antiferromagnetic alignment in (001) planes also occurs with a Néel temperature $T_N^{intra} > T_C^{inter}$. The *in*-plane antiferromagnetism can be commensurate or incommensurate with lattice periodicity. In the case of heavy rare-earth elements, there is only antiferromagnetic alignment of Mn moments along the *c* axis with the Néel temperature T_N^{inter}. The nature of magnetic couplings in these compounds within and between the Mn layers is closely related to the *in*-plane Mn–Mn spacing d^a_{Mn-Mn}. Roughly, if $d^a_{Mn-Mn} > 2.87$ Å ($a > 4.06$ Å), the *intra*layer *in*-plane coupling is antiferromagnetic and the *inter*layer coupling is ferromagnetic. When 2.84 Å $< d^a_{Mn-Mn} < 2.87$ Å (4.02 Å $< a < 4.06$ Å), the *intra*layer *in*-plane coupling is antiferromagnetic, but the *inter*layer coupling is also antiferromagnetic. In the case $d^a_{Mn-Mn} < 2.84$ Å ($a < 4.02$ Å), there is effectively no *intra*layer *in*-plane spin component and the *inter*layer coupling remains antiferromagnetic [4, 5].

Due to the strong dependence of the *inter*layer Mn–Mn exchange interaction on the lattice parameter a, one can vary the d^a_{Mn-Mn} value in the neighbourhood of the critical value by alloying different elements to RMn_2Ge_2, with R being a heavy rare-earth, and observe the destruction, stabilization and variation of different types of ferromagnetic and antiferromagnetic phases. In this paper, we have studied magnetic properties of $PrMn_2Ge_2$ compounds by substituting Gd for the light rare-earth Pr. This leads to the transition from parallel to antiparallel spin alignment in adjacent Mn layers. In such a study, it is possible to gain information on both the *intra*layer and *inter*layer magnetic properties of Mn planes [6, 7].

According to whether the sample is cooled with or without a low external field from the high-temperature AF phase to below the Curie temperature, the *inter*layer FM components are 'pinned' into different configurations by the AF component. It is then possible to identify the transitions from the field-cooled (FC) or zero-field-cooled (ZFC) data, or both, according to the magnitudes of the features present [7, 8]. In order to make use of the intrinsic pinning to characterize the various magnetic transitions, we performed low-field magnetization measurements on $Pr_{1-x}Gd_xMn_2Ge_2$. We also combine the results of magnetization measurements, earlier Mössbauer studies and neutron diffraction results on $PrMn_2Ge_2$ to give an account of the competing magnetic interactions [9–16]. Before proceeding to the presentation of the results, we give a brief outline of the magnetic properties of the end compositions below.

2. The magnetic properties of the end compositions

In $PrMn_2Ge_2$, the Mn sublattice orders antiferromagnetically in the *ab* plane below the Néel temperature $T_N^{intra} = 415$ K [10]. Cooling to temperatures below the 'Curie' temperature $T_C^{inter} \approx 330$ K leads to a canted spin structure with the *c* axis *inter*layer spin components aligning parallel [9]. Below 280 K, the magnetic structure transforms from a canted to a conical configuration with a cone semi-angle of approximately 58° [9]. The *c* axis *inter*layer alignment remains parallel. The Pr sublattices are magnetically disordered at these high temperatures and order along the *c* axis parallel to the Mn moments only below $T_C^{Pr} \approx 100$ K [9, 10]. The magnetic structure of the Mn sublattice below this temperature remains conical.

Neutron diffraction experiments are difficult to perform due to the large neutron absorption coefficient of Gd. In $GdMn_2Ge_2$, magnetization measurements have shown that the Mn moments are ordered antiferromagnetically below $T_N^{inter} = 365$ K, where the Gd moments remain disordered. Above this temperature, $GdMn_2Ge_2$ is a weak ferromagnet in a narrow temperature range and becomes paramagnetic above about 466 K [11–13, 17, 18]. A transition from antiferromagnetic ordering to a ferrimagnetic ordering takes place at 95 K with decreasing

temperature. From the Mössbauer study, it was concluded that $GdMn_2Ge_2$ is a collinear ferrimagnet below $T_C^{Gd} = 95$ K [18]. In the ferrimagnetic ordering, the Gd moments are ordered ferromagnetically along the *c* axis and all the Mn moments are aligned antiparallel to the Gd moment [12–14]. Another important feature of $GdMn_2Ge_2$ is a field-induced magnetic transition and a large positive magnetoresistance associated with the field-induced transition below 95 K [15].

3. Experimental details

Polycrystalline samples $Pr_{1-x}Gd_xMn_2Ge_2$ with $x = 0$, 0.2, 0.4, 0.65, 0.75, 0.8, 0.825, 0.85, 0.875, 0.9 and 1.0 were synthesized by arc melting the elements in a water-cooled Cu hearth under purified argon gas. The purity of the elements was 99.9% for Pr and 99.9% for Gd, 99.98% for Mn and 99.9999% for Ge. The mass loss of Mn during melting was compensated by adding 2% excess Mn. The ingots were melted five times to attain homogeneity.

The samples were characterized by powder x-ray diffraction on a Siemens D500 diffractometer using Cu Kα radiation and a secondary monochromator. The magnetization was measured using a SQUID magnetometer in the temperature range 5–350 K. The samples were first heated above T_C^{inter} and then measured in a ZFC–FC sequence. Magnetization above T_C^{inter} was measured with a vibrating sample magnetometer in an external magnetic field of 5 kOe.

4. Results

4.1. The structural properties

The x-ray diffraction patterns, obtained at room temperature, revealed the characteristic reflections of a tetragonal body-centred $ThCr_2Si_2$-type structure with space group $I4/mmm$ for all samples. For the samples with $x = 0.2$, 0.65, 0.8, 0.85 and 0.9 figure 1 displays the results of Rietveld refinements obtained at room temperature. The refined tetragonal lattice parameters a and c, the unit cell volume V and the *intra*layer Mn–Mn spacing d^a_{Mn-Mn} as a function of x are shown in figure 2. The critical *intra*layer spacings governing the nature of the Mn–Mn magnetic coupling are shown with the shaded areas in figure 2. The lattice parameters and the corresponding unit cell volume decrease monotonically with increasing Gd concentration. This behaviour is related to the smaller atomic size of Gd compared to that of Pr. As a consequence, the decrease of the lattice parameters results in the decrease of the *intra*layer Mn–Mn spacing d^a_{Mn-Mn} and *inter*layer nearest Mn–Mn distance.

4.2. The high temperature susceptibility

The temperature dependence of the magnetization in the range 300–610 K in an applied field of 5 kOe was measured to determine the Néel temperature of *intra*layer Mn alignment and is given in figure 3. The Néel temperature for $x = 0$, which is found from a change in slope of the inverse susceptibility of the compound, is at about 430 K [7]. This temperature is comparable with the Néel temperature $T_N^{intra} = 415$ K, which has been determined by magnetization measurements, neutron diffraction and Mössbauer studies for $PrMn_2Ge_2$ [9, 10, 16]. Therefore, T_N^{intra} for all other concentrations is also deduced from a change in the slope of inverse susceptibility. T_N^{intra} temperatures are designated by arrows in the high temperature magnetization curves. More details concerning this point are discussed in section 5.

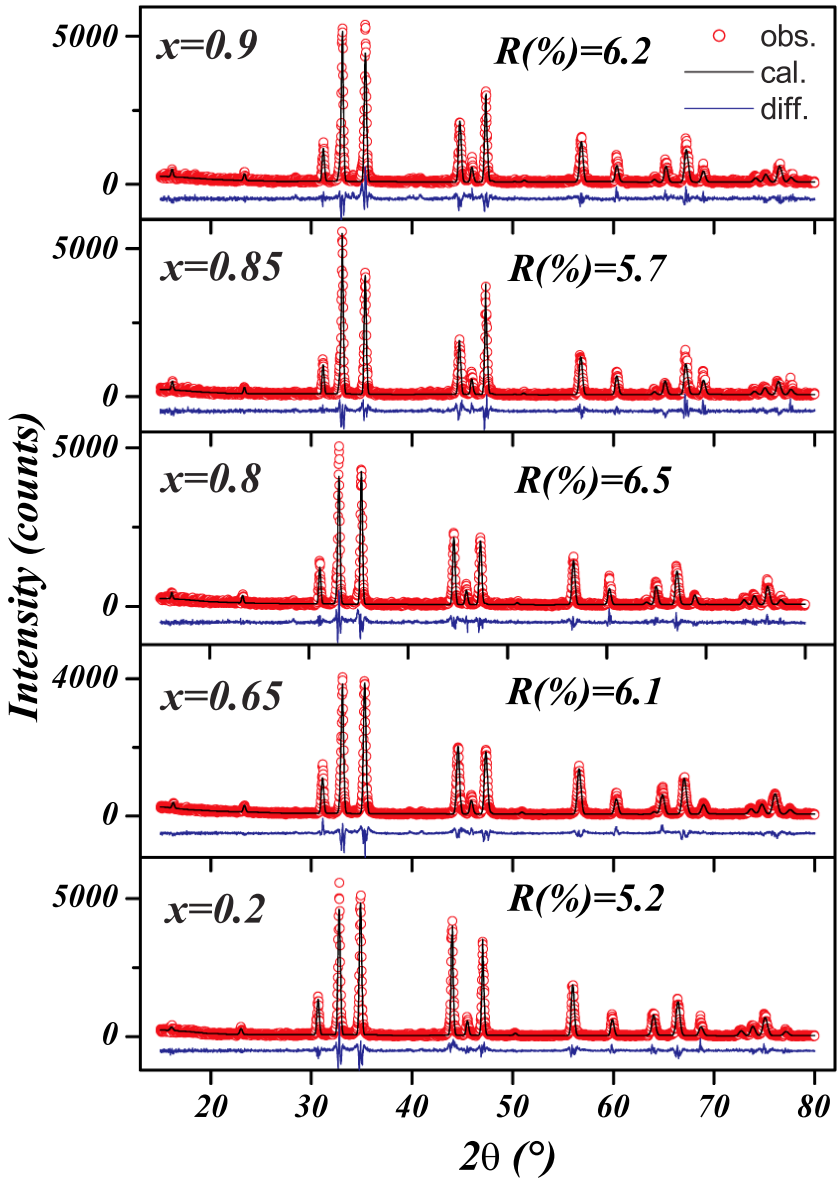

Figure 1. Rietveld refinements of the x-ray diffraction patterns of the samples with $x = 0.2$, 0.65, 0.8, 0.85 and 0.9. The points and the line refer to the recorded pattern and the calculated fit, respectively; the difference pattern is plotted in the lower part of the figure.

(This figure is in colour only in the electronic version)

4.3. Magnetization below 300 K

The results of magnetization measurements of $Pr_{1-x}Gd_xMn_2Ge_2$ compounds taken in an applied field of 50 Oe are shown in figure 4. Results of magnetization measurements as a function of temperature show qualitatively different behaviours for different compositions. The type of magnetic ordering above T_N^{intra} has been clarified by neutron diffraction [9] and

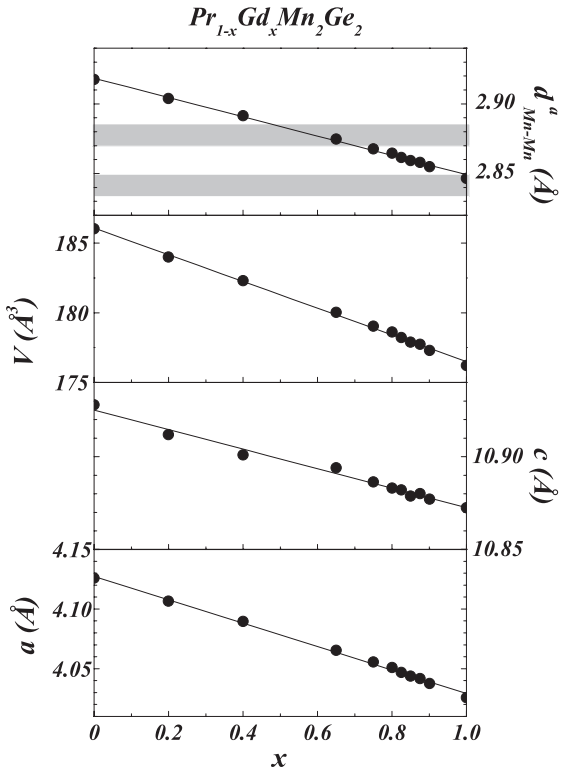

Figure 2. The concentration dependence of the lattice parameters a and c, the unit cell volume V and the *intra*layer Mn–Mn spacing $d^a_{\mathrm{Mn-Mn}}$.

Mössbauer studies [10] on $PrMn_2Ge_2$. Below the Néel temperature $T_{\mathrm{N}}^{\mathrm{intra}} \approx 430$ K, the ordering is found to be antiferromagnetic only in the Mn *intra*layer with moments in the (001) Mn planes. Below $T_{\mathrm{C}}^{\mathrm{inter}}$, the magnetization of the compounds with $x \leqslant 0.9$ increases rapidly with decreasing temperature, as expected for a system with ferromagnetic alignment of Mn moments along the c axis. This temperature, which is obtained from the inflection point of the derivative of magnetization, is close to the Curie temperature of the ferromagnetic alignment of the Mn sublattice for $x = 0$ and, therefore, the same criterion was applied for the other compounds. Upon cooling below $T_{\mathrm{C}}^{\mathrm{inter}}$, the data for $x = 0$ show a distinct feature at about 290 K both in the FC and ZFC states. This temperature is related to the temperature of the transition from the canted to the conical spin structure observed by neutron diffraction and is designated as $T_{\mathrm{c/c}}$ [9]. Similarly, $T_{\mathrm{c/c}}$ is found to be 260 K for $x = 0.2$. The distinct feature is not observed in $M(T)$ data of the other samples. An increase at $T_{\mathrm{C}}^{\mathrm{R}} = 100$, 80 and 66 K in the FC curve for the compounds with $x = 0$, 0.2 and 0.4, respectively, is attributed to the beginning of parallel ordering of the rare-earth sublattice to the Mn sublattice.

The lattice parameters for the $x \geqslant 0.65$ compounds are close to the critical values for ferromagnetic or antiferromagnetic coupling in the Mn sublattices (figure 2). At low temperatures, the magnetizations of these compounds show a progressive decrease with decreasing temperature. The overall magnetizations of the samples decrease with increasing x; this is related to the substitution of Gd for Pr which introduces more pronounced antiferromagnetic interactions between two Mn layers. Just below $T_{\mathrm{C}}^{\mathrm{inter}}$, the magnetization curves of the samples with $x = 0.825$, 0.85, 0.875 and 0.9 show ferromagnetic behaviour.

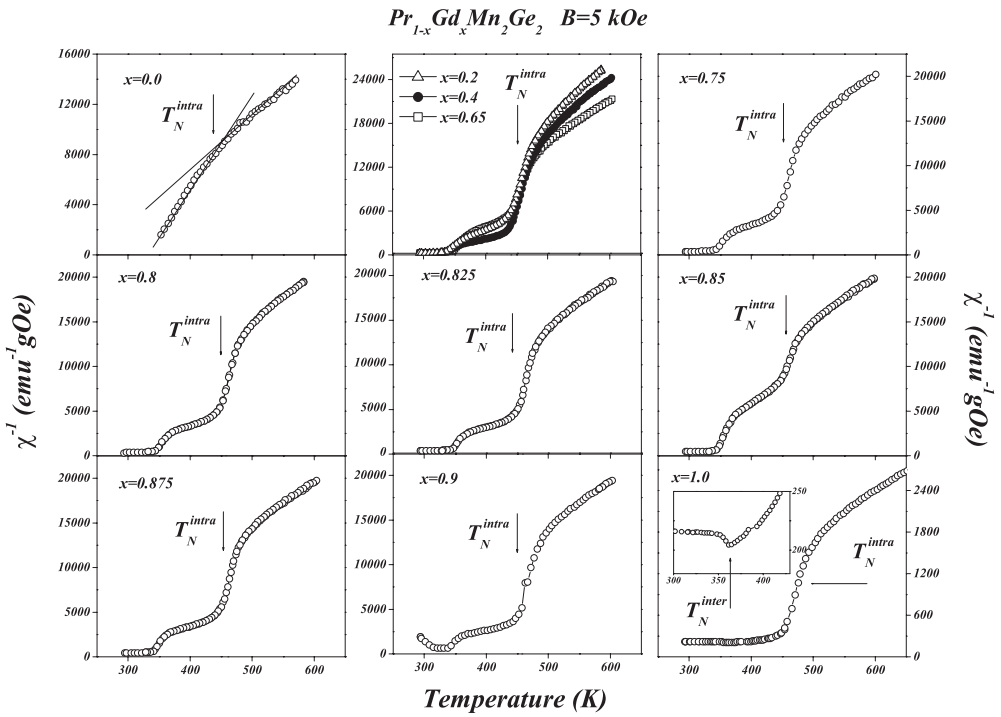

Figure 3. The temperature dependence of the magnetization of $Pr_{1-x}Gd_xMn_2Ge_2$ above 300 K in an applied field of 5 kOe (for $PrMn_2Ge_2$ a field of 1.2 kOe).

This ferromagnetic phase is related to the *inter*layer parallel alignment of the Mn spins along the c axis. The sample with $x = 0.825$ orders first ferromagnetically at T_C^{inter}, but because of lattice contraction on cooling further below T_C^{inter}, antiferromagnetic exchange is additionally introduced. Upon cooling, the magnetization decreases rapidly at 192 K and increases rapidly again at 163 K. It persists down to T_N^{inter}, where a transition to an antiferromagnetic phase occurs. In the antiferromagnetic region, the moments of the Mn layer are aligned antiparallel along the c axis. The antiferromagnetic temperature range broadens as the Gd concentration increases and the antiferromagnetic state becomes stable. This phase is stable down to T_C^R. Below T_C^R, these increases in $M(T)$ are attributed to the ordering of the rare-earth sublattice and the ordering of the rare-earth sublattice causes the Mn sublattice to order parallel along the c axis, so that the antiferromagnetism vanishes. This leads to the ferrimagnetic state, where the Gd moments align antiparallel to the Pr and Mn moments.

Since the lattice parameter a of the compound with $x = 1.0$ is greater than 4.02 Å at room temperature, according to the spacing condition, this compound should have a canted antiferromagnetic structure along the c axis below the $T_N^{inter} = 365$ K. Above this temperature, *intra*layer antiferromagnetism should occur.

Large differences between the FC and ZFC modes indicate a different configurational pinning for each mode of measurement. The *inter*layer ferromagnetic component is pinned by the anisotropy of the *intra*layer antiferromagnetic component of the Mn sublattice when the system is cooled through T_C^{inter} with or without an applied field [7]. Just below T_C^{inter}, a strong splitting is found for the samples with $x \leqslant 0.9$. Cooling from the antiferromagnetic state at $T_C^{inter} < T < T_N^{intra}$ and through T_C^{inter} in an external magnetic field gives a preferred orientation of the ferromagnetic components. In the ZFC case, a preferred orientation is not

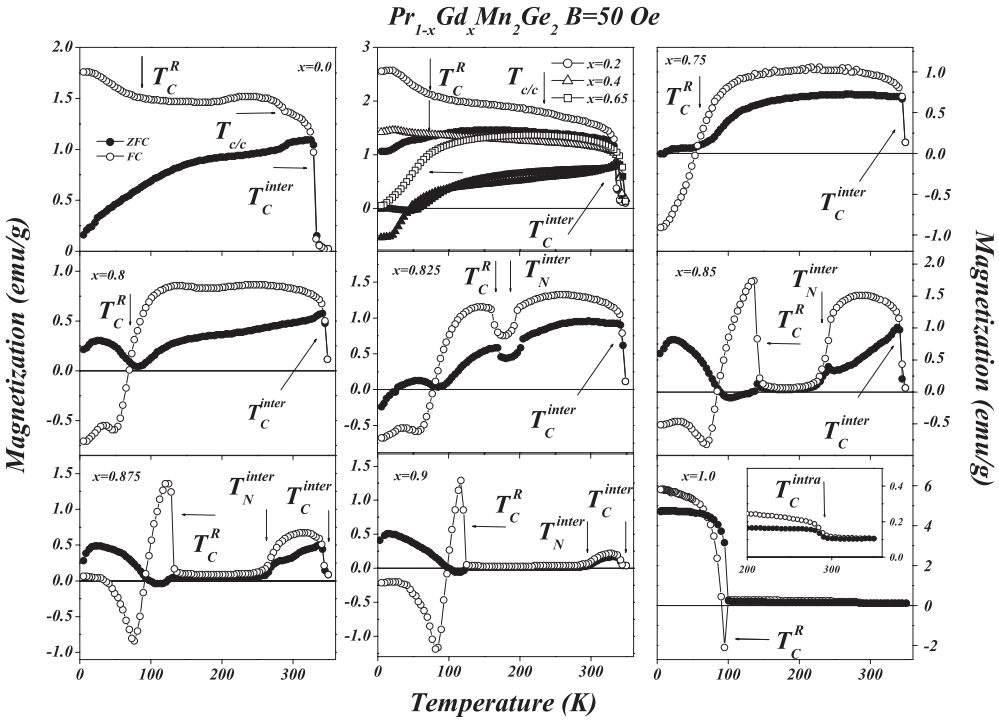

Figure 4. The temperature dependence of the magnetization of $Pr_{1-x}Gd_xMn_2Ge_2$ in an applied field of 50 Oe (for $Pr_{0.1}Gd_{0.9}Mn_2Ge_2$ of 20 Oe). For the samples with $0 \leqslant x \leqslant 0.9$, the splitting in $M(T)$ of the ZFC and FC states below the Curie temperature T_C^{inter} can be attributed to different configurational pinning of the ferromagnetic component by the *intra*layer antiferromagnetism. The negative values of the magnetizations for the Gd-rich compounds at low temperatures are related to the opposite alignment of Gd moments to the direction of the weak magnetic field. Similar behaviour is also observed for the Tb-rich compounds in $Pr_{1-x}Tb_xMn_2Ge_2$ at low temperatures for an applied field of 100 Oe and the values of magnetizations of the same compounds are positive for an applied field of 1 kOe [7].

induced and, therefore, the total magnetization is weaker than in the FC. In both cases, the *inter*layer ferromagnetic components are pinned by the higher anisotropy of the *intra*layer antiferromagnetic component. Such a pinning effect is not observed for $x > 0.9$. By making use of this effect, T_C^{inter} can be determined with good precision. The transition temperatures of all the samples are listed in table 1.

5. Discussion

Since neutron diffraction experiments are difficult to perform due to the high absorption of Gd, no neutron diffraction study has been performed on $GdMn_2Ge_2$. From the present magnetization data and earlier magnetization and Mössbauer studies on $PrMn_2Ge_2$ and $GdMn_2Ge_2$ and a neutron study on $PrMn_2Ge_2$, we construct the magnetic phase diagram of $Pr_{1-x}Gd_xMn_2Ge_2$. The complexity of the magnetization data does not allow for a clear-cut identification of each transition temperature. Therefore, the diagram has to be constructed self-consistently starting from the end concentrations and eventually approaching the intermediate ones and, then, rechecking if the obtained transition temperatures are consistent among themselves. The resulting phase diagram with such a refinement is shown in figure 5, and its construction is presented below.

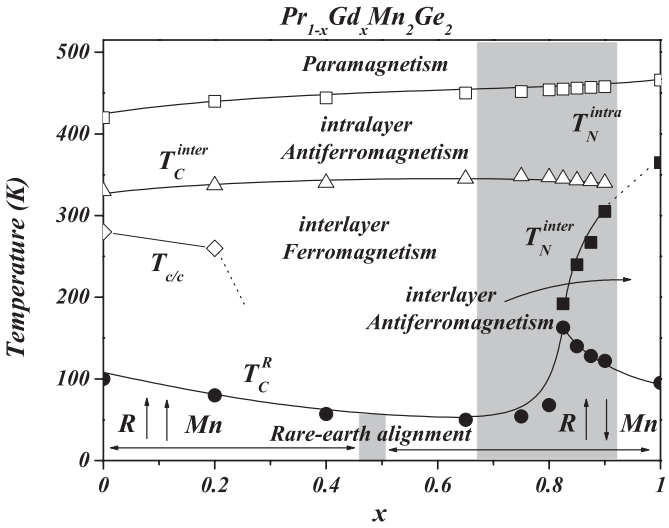

Figure 5. Proposed magnetic phase diagram of $Pr_{1-x}Gd_xMn_2Ge_2$. The magnetic structures of the various regions have been labelled according to the magnetic transition temperatures in table 1. The broken lines drawn in the diagram are extrapolations.

Table 1. The magnetic transition temperatures. T_C^{inter} is the ferromagnetic ordering temperature of Mn sublattices along the *c* axis. T_N^{inter} is the antiferromagnetic ordering temperature of Mn sublattices along the *c* axis. T_C^R is the ferromagnetic ordering temperature of rare-earth sublattices along the *c* axis. T_N^{intra} is the antiferromagnetic ordering temperature of Mn sublattices within (001) Mn planes. $T_{c/c}$ is the transition temperature from canted ferromagnetism to conical ferromagnetism for Mn sublattices. T_{comp} is the compensation temperature of the ferrimagnetism below T_C^R. T_C^{intra} is the ferromagnetic ordering temperature of Mn sublattices within (001) Mn planes.

x	T_C^{inter} (K)	T_N^{inter} (K)	T_C^R (K)	T_N^{intra} (K)	$T_{c/c}$ (K)	T_{comp} (K)	T_C^{intra}
0.0	330		100	420	280		
0.2	337		80	440	260		
0.4	340		60	444			
0.65	345		55	450			
0.75	348		53	452		54	
0.8	347		65	454		80	
0.825	345	192	163	455		79	
0.85	343	240	140	455		84	
0.875	340	267	128	457		91	
0.9	340	305	122	458		98	
1.0		365	95	466			290

5.1. The high temperature susceptibility

The nature of magnetic ordering between T_C^{inter} and T_N^{intra} of $PrMn_2Ge_2$ has been studied extensively by neutron diffraction and Mössbauer studies [9, 10]. From these studies on $PrMn_2Ge_2$, 430 K corresponds to the Mn *intra*layer *in*-plane antiferromagnetic ordering temperature T_N^{intra}. The value $T_N^{intra} = 430$ K for $PrMn_2Ge_2$ obtained from figure 3 is identical to this value. Therefore, the features in figure 3 are expected to be associated with T_N^{intra} for all other concentrations as well. However, it was previously reported that $GdMn_2Ge_2$ is a

weak ferromagnet between 365 and 466 K [11–13, 17, 18]. On the other hand, Nowik *et al* concluded from their ^{57}Fe Mössbauer measurements on $GdMn_2Ge_2$ at 375 K that the compound is paramagnetic [10, 19]. The magnetization of $Pr_{1-x}Gd_xMn_2Ge_2$ at high temperatures shows features related to a magnetic transition around $T_N^{intra} \approx 460$ K (figure 3). These features, observed in $M(T)$ or $\chi^{-1}(T)$, are expected to be associated with the onset of the Mn *intra*layer antiferromagnetic coupling.

5.2. Magnetization below 300 K

The substitution of Gd for Pr causes a decrease in the Mn–Mn *intra*layer distance and a depression of ferromagnetic ordering of the Mn planes. The overall magnetization decreases with increasing Gd concentration and ferromagnetic Mn planes begin to align antiparallel along the c axis. This is seen in the systematic decrease of the absolute value of the magnetization just below T_C^{inter} as the Gd concentration increases. Although the magnetization decreases, T_C^{inter} is almost concentration-independent up to $x = 0.9$ and above this concentration the ferromagnetism vanishes almost abruptly and antiferromagnetism sets in. This behaviour indicates that the magnetic exchange is little affected by the change from ferromagnetic to antiferromagnetic. At around 280 K, the magnetization of the $x = 1.0$ sample shows an increase in the FC and ZFC states with decreasing temperature, as clearly seen in figure 4. This increase and splitting between FC and ZFC curves indicate a weak ferromagnetic component. Above 280 K, there is a canted antiferromagnetic ordering along the c axis. The increase at this temperature may be related to the ferromagnetic ordering along the a or b axes which arises from a small angle between the antiferromagnetic component and the a or b axes in the ab plane. This temperature is designated as T_C^{intra} in table 1.

From the Pr-rich end of the diagram up to $x = 0.9$, the ab-plane antiferromagnetic state transforms to a ferromagnetic state with decreasing temperature. For $x = 0.0$ and 0.2, the ferromagnetic structure along the c axis is canted, and at $T_{c/c}$ the canted ferromagnetism transforms into a conical ferromagnetic state. The $T_{c/c}$ temperature was not observed for the other samples.

According to the spacing conditions the lattice parameters of the compounds with $x > 0.65$ are close to the critical values for ferromagnetic or antiferromagnetic coupling of the Mn sublattice. The area corresponding to these concentrations is shaded in the phase diagram. These samples order first ferromagnetically at T_C^{inter}, but because of lattice contraction on cooling further below T_C^{inter}, antiferromagnetic exchange is additionally introduced. The $x = 0.825$ sample lies at a near-critical concentration incorporating a mixture of *inter*layer ferromagnetic ordering and antiferromagnetic ordering. This reduction in ferromagnetic coupling continues as the Gd concentration increases and becomes an *inter*layer antiferromagnetic state at a low enough temperature. The antiferromagnetic phase region expands with the Gd concentration. At lower temperatures, the rare-earth sublattice begins to order, as seen by the rapid increase with decreasing temperature in the FC magnetization. The temperature T_C^R is obtained from the inflection point of the derivative of the magnetization. Below T_C^R, the average moment of the Gd-rich rare-earth sublattice is aligned antiparallel to the Mn and Pr moments and the system enters a ferrimagnetic phase. For the Gd-rich samples the ferromagnetic ordering is dominant while for Pr-rich samples it is the ferromagnetic ordering below T_C^R (see figure 5).

The phase diagram which is proposed in figure 5 does not contain all the information on the various magnetic structures. To determine all the information about the possible magnetic structures, neutron diffraction experiments are required.

References

[1] Szytula A and Leciejewicz J 1989 *Handbook on the Physics and Chemistry of Rare Earths* vol 12, ed K A Gschneidner Jr and L Erwin (Amsterdam: Elsevier) p 133
[2] Szytula A 1991 *Handbook of Magnetic Materials* vol 6, ed K H J Buschow (Amsterdam: Elsevier) p 85
[3] Navashimhan K S V L, Rao V U S, Wallace W E and Pop I 1976 *AIP Conf. Proc.* **29** 594
[4] Szytula A and Siek S 1982 *J. Magn. Magn. Mater.* **27** 49
[5] Venturini G, Welter R, Ressouche E and Malaman B 1995 *J. Magn. Magn. Mater.* **150** 197
[6] Elerman Y, Kervan S, Duman E and Acet M 2002 *J. Magn. Magn. Mater.* **251** 251
[7] Duman E, Acet M, Elerman Y, Elmali A and Wassermann E F 2002 *J. Magn. Magn. Mater.* **238** 11
[8] Nowik I, Felner I and Bauminger E R 1997 *Phys. Rev.* B **55** 3033
[9] Welter R, Venturini G, Ressouche E and Malaman B 1995 *J. Alloys Compounds* **218** 204
[10] Nowik I, Levi Y, Felner I and Bauminger E R 1995 *J. Magn. Magn. Mater.* **147** 373
[11] Iwata N, Ikeda T, Shigeoka T, Fujii H and Okamoto T 1986 *J. Magn. Magn. Mater.* **54–57** 481
[12] Shigeoka T, Fujii H, Fujiware H, Yagosaki K and Okamoto T 1983 *J. Magn. Magn. Mater.* **31–34** 209
[13] Kobayashi H, Onodera H and Yamamoto H 1989 *J. Magn. Magn. Mater.* **79** 76
[14] Iwata N, Hattori K and Shigeoka T 1986 *J. Magn. Magn. Mater.* **53** 318
[15] Wada H, Yoshioka H and Goto T 2002 *J. Phys.: Condens. Matter* **14** L687
[16] Venturini G 1996 *J. Alloys Compounds* **232** 133
[17] Kervan S, Acet M and Elerman Y 2001 *J. Alloys Compounds* **312** 35
[18] Kervan S, Acet M and Elerman Y 2001 *Solid State Commun.* **119** 95
[19] Sanchez J P, Tomala K and Szytula A 1991 *Solid State Commun.* **78** 419